12-2018

Confined Fluid Analyzed with Near-field Acoustic Detection

Rodolfo Fernandez Rodriguez
Portland State University, rodolfo.f.r@gmail.com

Theodore Brockman
Portland State University

J. Bai
Portland State University

Andres H. La Rosa
Portland State University, andres@pdx.edu

Citation Details

Fernandez, R., Brockman, T., Bai, J., & La Rosa, A. H. (2018, December). Confined Fluid Analyzed with Near-field Acoustic Detection. In Journal of Physics: Conference Series (Vol. 1143, No. 1, p. 012017). IOP Publishing.

Confined Fluid Analyzed with Near-field Acoustic Detection

IOP Conf. Series: Journal of Physics: Conf. Series **1143** (2018) 012017 doi:10.1088/1742-6596/1143/1/012017

Confined Fluid Analyzed with Near-field Acoustic Detection

R Fernandez, T Brockman, J Bai and A H La Rosa

Portland State University, Portland, Oregon 97201, USA

E-mail: andres@pdx.edu

Abstract. Measurement of the damping and elastic interactions between two solids interfaces (one being the apex of a tapered probe that is attached to one tine of a quartz tuning fork while the other is a flat substrate) under relative lateral oscillatory motion are reported. The solid boundaries are separated by a nanometer sized gap, and emphasis is placed on the role played by the mesoscopic fluid trapped in between. The measurements were implemented using two new acoustic techniques that have been integrated into a tuning fork based scanning probe microscope; the whole metrology system offers sub-nanometer precision for controlling the probe's vertical position, as well as thermal drift correction. One of the acoustic techniques, Shear-force Acoustic Near-field Microscopy (SANM), monitors the acoustic emission from the trapped fluid subjected to shear stress, while Whispering Gallery Acoustic Sensing (WGAS) monitors the oscillation amplitude of the QTF. Additionally, the elastic and damping components of the probe-fluid interaction forces are decoupled by operating the SANM in frequency modulation mode, while the eventual contact between the probe and substrate is tracked by monitoring the electrical current signal. Results involving interaction in the 0 to 5 nN regime are reported. The measurements reveal a strong correlation between the monotonic shift of the probe's resonance frequency and the near-field acoustic emission from the trapped fluid. The SANM signal, then, accounts as one of the elastic energy dissipation channels involved in surface interactions at ambient conditions.

1. Introduction

The physical properties of mesoscopic fluids found adsorbed at substrates or confined between solid surfaces differ greatly from those measured in their bulk form[1-3]. For example, the effective shear viscosity is enhanced, viscoelastic relaxation times are prolonged [4], they reveal different phase diagram[5] (boiling at lower temperatures, ice formation at room temperature[6, 7]), the so called hydrophobic interaction manifests at distances well beyond commonly accepted molecular interaction ranges[8], interfacial adhesion[9], molecular transport in nanostructures[10, 11], molecular assembly of particles in liquid water[12, 13] and filtration[14]. But the physics of such a unique dynamic behavior displayed by mesoscopic fluid films still lacks a comprehensive description.

Herein we report the use of a new acoustic metrology tools, Shear-force Acoustic Near-field Microscopy (SANM)[15,16] and Whispering Gallery Acoustic Sensing (WGAS)[17], to characterize the dynamics of fluid films trapped between solid surfaces in relative motion. Figure 1a illustrates the particular physical situation being addressed. When the apex of a laterally-oscillating tapered probe is placed close enough to a flat substrate, a water bridge suddenly forms between the probe and the substrate; the latter occurs at a distance that varies stochastically (from few nanometers to tens of nanometers) depending on the wetting properties of the probe and the substrate, environmental humidity, and temperature. It is of interest to find out the elastic (k_{fluid}) and damping (γ_{fluid}) properties of the trapped fluid for different probe-

substrate separation distances. We report here a correlation between the fluid's acoustic emission and the frequency shift of the probe's resonance frequency.

2. About the new SANM and WGAS acoustic techniques

The development of SANM and WGAS was initially triggered by an interest for understanding the principles underlying *wear-free friction phenomena,* also referred here as *Interfacial friction.* The use of a tapered probe, as one of the interacting surfaces, is to study the problem at nanoscale dimensions.

i) Could it be that part of the energy is dissipated via acoustic emission (*i.e*. energy is dissipated in the form of sound waves emitted by the confined fluid, which then couples to the substrate underneath)? To address this question we place an acoustic transducer (the SANM acoustic sensor) in intimate contact with the bottom side of the substrate (as shown in figure 1b), to thus listen to the eventual fluid's acoustic emission[15-18]. To set the probe's apex into lateral motion, the probe is glued to one of the tines of a quartz tuning fork (QTF); an ac-voltage sets the tines of the QTF into lateral oscillatory motion. This way, adhesion interactions at the probe-fluid interface causes to set the fluid into shear motion.

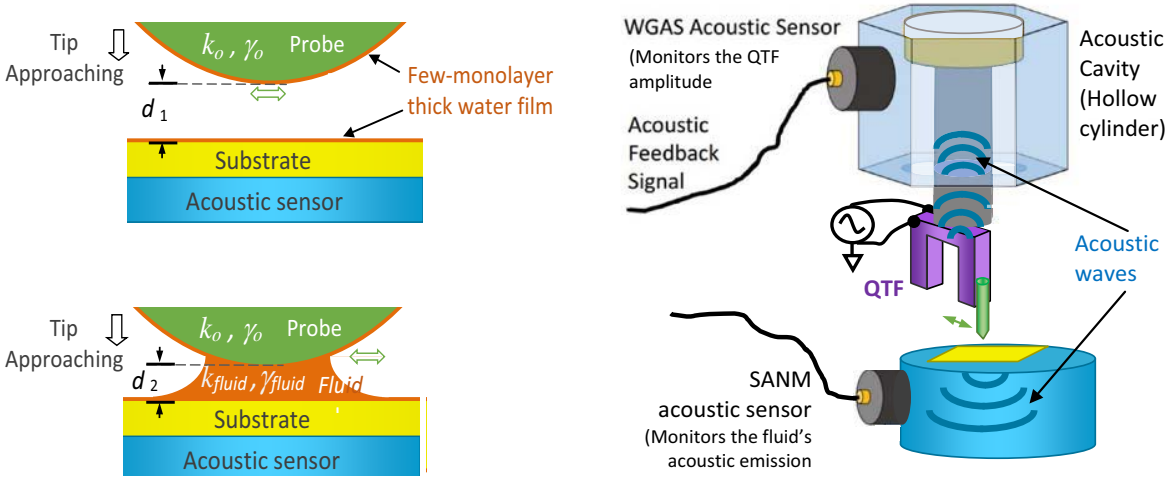

Figure 1. Left: Spontaneous formation of fluid bridge when a laterally oscillating probe approaches the substrate. The confined fluid undergoes shear interaction with the probe. Finding the fluid's viscoelastic properties (k_{fluid}, γ_{fluid}) of this fluid constitutes the subject of our studies. **Right:** The central part shows a probe attached to a QTF, which is electrically driven at its resonance frequency. In the upper part, the WGAS sensor monitors the probe's mechanical response. In the lower part, the SANM sensor monitors the confined fluid acoustic emission.

ii) Shouldn't such a fluid's elastic response (the acoustic emission) have a counterpart reaction on the probe, like a change in its resonance frequency, as well as a decrease in the probe's amplitude of oscillations? Such changes in the probe's amplitude and frequency shift can be addressed with any typical scanning probe microscopy. Here, however, we highlight a new contactless acoustic method (WGAS) to monitor the probe's motion. In effect, without disturbing the probe motion, we simply place an acoustic transducer at a strategic location around the microscope's frame, away from the probe (figure 1b)[17]. The suggested underlying mechanism is that the lateral motion of the tines sets an internal acoustic wave that travels up the central shaft holder (see figure 1b), and subsequently establishes stationary waves in the

cylindrical frame cavity. An acoustic sensor, strategically placed at one acoustic node on the periphery of the cavity, picks a signal that, it turns out, correlates linearly with the probe's amplitude. The WGAS measurements offer nanometer amplitude sensitivity.

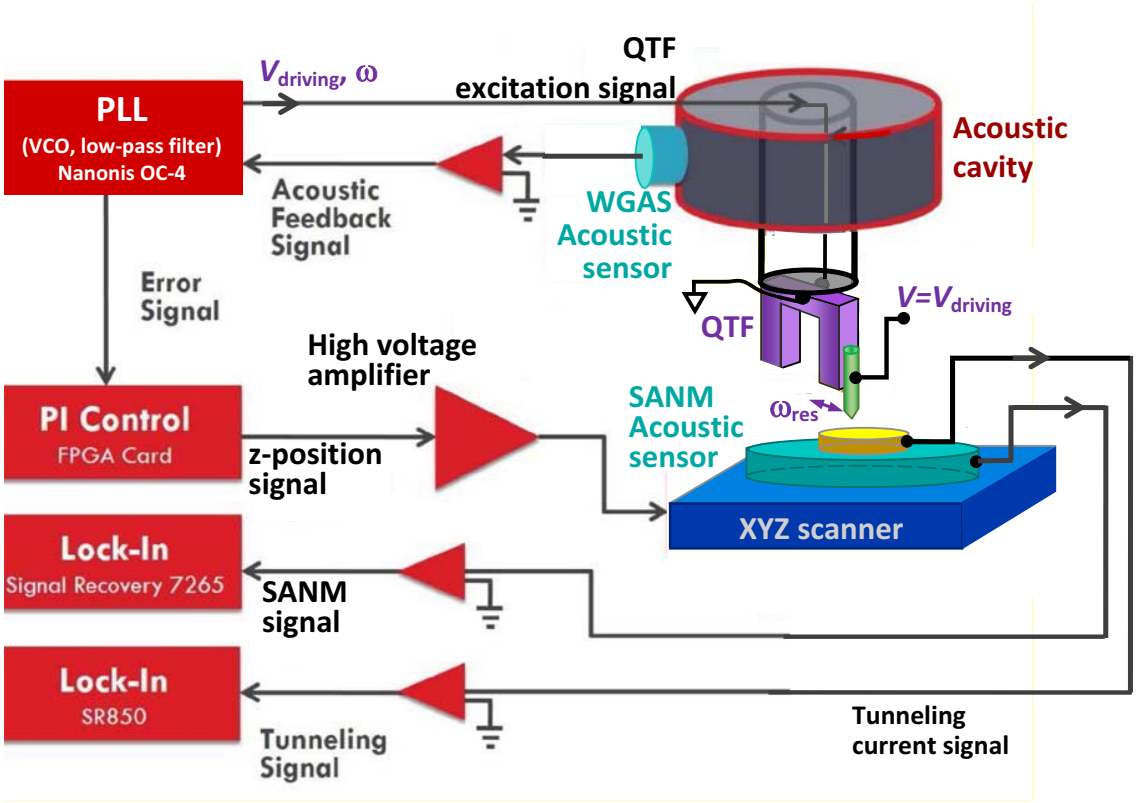

Figure 2. Probe-substrate distance regulation implemented with phase-lock-loop (PLL) frequency modulation. The PLL uses the WGAS as a feedback signal control. This setting allows driving the QTF at resonance at all times, while the probe's apex interacts with the fluid bridge. Several signals are monitored concurrently as the probe approaches the substrate: the probe's amplitude (WGAS), the acoustic emission from the trapped fluid (SANM), the shift in the probe's resonance frequency, and the tunneling current to establish the contact between the probe and the substrate. In the latter, the voltage driving the QTF is also used as bias voltage on the tip to measure the tunneling current.

3. Position control in frequency modulation modality using WGAS as a feedback control signal

Further, frequency modulation detection is also integrated into the SANM/WGAS system (figures 2 and 3) in order to discriminate the damping from the elastic forces components. This is an outgrowth of the single frequency excitation scheme depicted in Fig. 1, where a decrease in the probe's amplitude can be attributed to not only damping effects but also due the fact the resonance frequency of the probe changes as the probe-substrate distance decreases. A frequency modulation strategy overcomes this shortcoming. Succinctly, during a probe's trip approach, once the apex starts interacting with a mesoscopic fluid (assumed viscoelastic), the WGAS sinusoidal output signal (acoustic feedback signal in figure 2) undergoes a phase change because the probe is now out of resonance. Such a change in phase is utilized by the PLL section, where a voltage controlled oscillator (VCO) responds by adjusting the frequency (ω) of the output driving

voltage (V_{driving}) until the laterally oscillating probe reaches again the resonance condition (*i.e*. the phase of the WGAS signal is back to its initial phase resonance condition) at the new probe-substrate distance. This way, *i*) changes in the probe's amplitude can be ascribed solely to damping effects; and *ii*) the change in the resonance frequency gives a direct measurement of the elastic component of the probe-fluid interaction. We emphasize the PLL-SANM settings shown in figures 2 and 3 use the WGAS acoustic signal as the control signal. Its selection over the electrical QTF response is that WGAS offers an alternative way to more accurately monitor the QTF mechanical oscillations (the latter not always correlates with the QTF electrical response.)

4. Retrieving viscoelastic properties from changes in resonance frequency shifts and variations in the probe's amplitude.

The use of a quartz tuning fork in the SANM is to capitalize on its very-low energy-dissipation property (one obtains a mechanical Q factor above 2,500 even after mounting a tapered probe), which also allows describing its mechanical response through a simple harmonic oscillator (SHO) model[19,20]. The predicted linear dependence between Q and the QTF oscillation amplitude (while a tip, attached to one of its tines, interact with a mesoscopic fluid at different probe-substrate distances) has been verified[21]. This has impelled using the SHO model also in frequency modulation methods to extract effective values of the fluid's viscoelastic parameters k_{fluid} and γ_{fluid} affecting the TF oscillatory motion[22]. This is obtained by comparing the equation of motion that describes the probe's apex interacting with a viscoelastic fluid layer $M\ddot{x} + M(\gamma_o+\gamma_{fluid})\dot{x} + (k_o+k_{fluid})x = Fe^{i\omega t}$, with the one when the probe is far away from the substrate $M\ddot{x} + M\gamma_o\dot{x} + k_o x = Fe^{i\omega t}$. The equations are deceptively simple but k_{fluid} and γ_{fluid} can be a complicated function of several parameters, including temperature, pressure, and speed of the probe's motion[23].

In figure 1a, k_o and γ_o constitute, respectively, the elastic spring constant and the (intrinsic) damping constant of the QTF (with the tapered probe attached to one of its tines). Let's denote $x_\infty = x_\infty(t)$ as the lateral probe's position variable when the distance between the probe and sample is infinite,

$$M\,\ddot{x}_\infty + M\gamma_o\,\dot{x}_\infty + k_o\,x_\infty = Fe^{i\omega t} \quad (1)$$

$$x_\infty = A_\infty(\omega)\, e^{i\omega t} \quad (2)$$

$$[\,-M\,\omega^2 + i\omega M\,\gamma_o + k_o\,]\,A_\infty(\omega) = F \quad (3)$$

Using $\omega_{res,\infty}$, the resonance frequency of the probe when the probe-substrate distance is ∞,

$$\omega_{res,\infty}{}^2 \equiv k_o/M \quad (4)$$

one obtains,

$$M\,[\,-\omega^2 + i\omega\,\gamma_o + \omega_{res,\infty}{}^2\,]\,A_\infty(\omega) = F$$

At resonance condition, when $\omega = \omega_{res,\infty}$,

$$M\,[\,i\,\omega_{res,\infty}\;\gamma_o\,]\,A_\infty(\omega_{res,\infty}) = F \quad (5)$$

When the probe is placed near the substrate a meniscus is formed, whose effect on the probe's motion is quantified by an additional damping $\gamma_{fluid,d}$ and elastic $k_{fluid,d}$ parameters. When the probe-substrate separation is *d*, let's denote by x_d the variable monitoring the probe's lateral position,

$$M\ddot{x}_d + M(\gamma_o + \gamma_{fluid,d})\dot{x}_d + (k_o + k_{fluid,d})\, x_d = Fe^{i\omega t} \quad (6)$$

$$x_d = A_d(\omega)\, e^{i\omega t} \quad (7)$$

$$[\, -M\omega^2 + i\omega M(\gamma_o + \gamma_{fluid,d}) + (k_o + k_{fluid,d})\,]\, A_d(\omega) = F \quad (8)$$

Using $\omega_{res,d}$, the resonance frequency of the probe when the probe-substrate distance is *d*,

$$\omega_{res,d}{}^2 \equiv (k_o + k_{fluid})/M \quad (9)$$

one obtains,

$$M[\, -\omega^2 + i\omega(\gamma_o + \gamma_{fluid,d}) + \omega_{res,d}{}^2\,]\, A_d(\omega) = F \quad (10)$$

At resonance condition, when $\omega = \omega_{res,d}$

$$M\, i\, \omega_{res,d}\, [\gamma_o + \gamma_{fluid,d}]\, A_d(\omega_{res,d}) = F \quad (11)$$

From (4) and (9),

$$\omega_{res,d}{}^2 \equiv \omega_{res,\infty}{}^2 + k_{fluid,d}/M$$

$$k_{fluid,d} = M[\, \omega_{res,d}{}^2 - \omega_{res,\infty}{}^2]$$

$$= M\, \omega_{res,\infty}{}^2 [\, \frac{\omega_{res,d}{}^2}{\omega_{res,\infty}{}^2} - 1]$$

$$k_{fluid,d} = k_o [\, \frac{\omega_{res,d}{}^2}{\omega_{res,\infty}{}^2} - 1] \quad (12)$$

From (5) and (11),

$$M[\, i\, \omega_{res,\infty}\, \gamma_o\,]\, A_\infty(\omega_{res,\infty}) = M\, i\, \omega_{res,d}\, [\gamma_o + \gamma_{fluid,d}]\, A_d(\omega_{res,d})$$

$$[\, \frac{\omega_{res,\infty}}{\omega_{res,d}}\, \gamma_o\,]\, \frac{A_\infty(\omega_{res,\infty})}{A_d(\omega_{res,d})} = [\gamma_o + \gamma_{fluid,d}]$$

$$\gamma_{fluid,d} = \gamma_o[\, \frac{\omega_{res,\infty}}{\omega_{res,d}}\, \frac{A_\infty(\omega_{res,\infty})}{A_d(\omega_{res,d})} - 1] \quad (13)$$

Alternatively, in terms of the *Q* factor measured when the probe is far away from the substrate,

$$\gamma_{fluid,d} = \frac{\omega_{res,\infty}}{Q}[\, \frac{\omega_{res,\infty}}{\omega_{res,d}}\, \frac{A_\infty(\omega_{res,\infty})}{A_d(\omega_{res,d})} - 1]$$

$$= \frac{k_o}{MQ\, \omega_{res,\infty}}[\, \frac{\omega_{res,\infty}}{\omega_{res,d}}\, \frac{A_\infty(\omega_{res,\infty})}{A_d(\omega_{res,d})} - 1] \quad (14)$$

Expressions (12) and (13) gives the elastic and damping constants of the fluid in terms of,

$$A_d(\omega_{res,d}) \qquad \textit{the probe's resonant amplitude}, \tag{15}$$

and

$$\Delta\omega = (\omega_{res,d} - \omega_{res,\infty}) \qquad \textit{the probe's frequency shift,} \tag{16}$$

measured at different probe-substrate distance d.

From expression (8), the contribution from the fluid to the elastic force acting on the probe, measured at resonance condition, is given by,

$$F_{elast} = k_{fluid,d}\, A_d(\omega_{res,d})$$

$$F_{elast} = k_o\left[\frac{\omega_{res,d}^2}{\omega_{res,\infty}^2} - 1\right] A_d(\omega_{res,d}) \tag{17}$$

From expression (8), the contribution from the fluid to the damping force acting on the probe, measured at resonance condition, is given by,

$$F_{damp} = i\omega_{res,d}\; M\,\gamma_{fluid,d}\; A_d(\omega_{res,d}) \tag{18}$$

Alternatively, using (14),

$$F_{damp} = i\omega_{res,d}\; \frac{k_o}{Q\,\omega_{res,\infty}}\left[\frac{\omega_{res,\infty}}{\omega_{res,d}}\,\frac{A_\infty(\omega_{res,\infty})}{A_d(\omega_{res,d})} - 1\right] A_d(\omega_{res,d})$$

$$F_{damp} = i\,\frac{k_o}{Q}\,\frac{\omega_{res,d}}{\omega_{res,\infty}}\left[\frac{\omega_{res,\infty}}{\omega_{res,d}}\,\frac{A_\infty(\omega_{res,\infty})}{A_d(\omega_{res,d})} - 1\right] A_d(\omega_{res,d}) \tag{19}$$

When measuring the full width at half maximum $\Delta\omega$ from a $A_\infty^2(\omega)$ vs ω spectrum, the mechanical quality factor is estimated to be $Q = \omega_{res,\infty}/\Delta\omega$. If the full width at half maximum $(\Delta\omega)'$ is measured from a $A_\infty(\omega)$ vs ω spectrum, then, it turns out,

$$Q = \sqrt{3}\,\frac{\omega_{res,\infty}}{(\Delta\omega)'} \tag{20}$$

Since in the definition of the quality factor, $Q=\omega_{res,\infty}/\Delta\omega$, the value of $\Delta\omega$ turns out to be equal to γ_o, then expression (2) can be written as $F= M\,[\, i\,\omega_{res,\infty}^{\,2}/Q\,]\,A_\infty(\omega_{res,\infty})$, or $F=ik_o/Q\;A_\infty(\omega_{res,\infty})$. This expression allows estimating then the magnitude of the driving force,

$$F= \frac{k_o}{Q}\,\left|A_\infty(\omega_{res,\infty})\right| \tag{21}$$

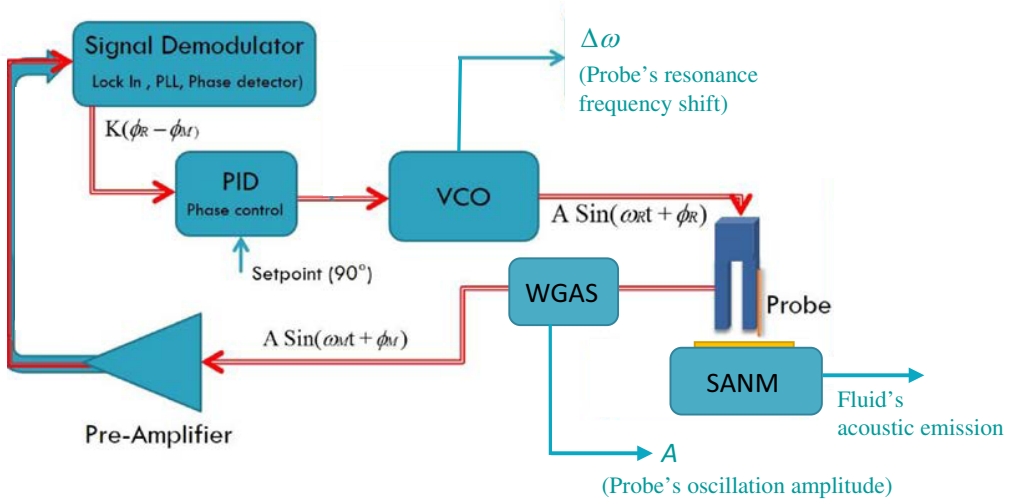

Figure 3. Implementation of frequency modulation to discriminate the elastic (via Δf detection) and damping component (via amplitude A detection) of the probe-fluid interactions. The amplitude and phase of the probe's motion are monitored by the WGAS system. The PLL demodulates the phase information, which is compared with set point of a PID phase control. Any deviation of the probe's phase from 90º triggers the VCO response to drive the QTF at different frequency until resonance condition is re-established.

5. Testing probe-fluid interactions in the low interaction forces regime (up to 5 nN)

A highly ordered pyrolitic graphite (HOPG) sample (7 mm X 7 mm x 1 mm SPI-2 grade, of resistivity values $\rho_{\perp}$ = 0.5 ohm-cm and $\rho_{//}$ = 0.5 x10^{-3} ohm-cm, from SPI Supplies, West Chester, PA) was secured with carbon conductive tape to the sample stage of the SANM. The sample was then cleaved with scotch tape. The QTF (with the probe attached) displayed a mechanical quality factor of Q=5,700; estimated oscillating amplitude of 26 nm (using a driving voltage V_{driving}=10 mV rms, see Fig. 2); resonance frequency $f_{res,\infty}$ = 31804 Hz; 117 nN driving force, as calculated from equation (21). The experiments were performed at 35 % relative humidity and 26 °C temperature.

The results reported here correspond to one of the first approaches of the probe towards the sample. On purpose, the approach stopped once the elastic interaction reached 5 nN, just to ensure an interaction of the probe with just the mesoscopic fluid (and aiming to avoid potential crash with the substrate). This implied, as displayed by the results, a decrease of the probe amplitude by 10% of its initial maximum amplitude. From previous results in our lab, the expected SANM signal at this shallow interaction condition should be very small (sometime undetected); hence the reason for driving the signal with a large amplitude (26 nm) larger than the usual 4 nm to 10 nm range used in previous experiments.

Figure 4 compares the WGAS signal (probe's amplitude of oscillations, expressed in percentage values), the normalized acoustic SANM magnitude (the normalization factor is the probe's amplitude of oscillations,) the acoustic SANM phase, and the damping force exerted by the fluid on the probe (calculated from expression (19),) all simultaneously obtained as the probe approaches the sample. The sudden small decrease in the probe's amplitude at 100 Å in Fig. 4 suggests the incipient (precursor) formation of finger-like bridges between the asperities on probe's apex and the sample [24]; the latter constituting also a vehicle for establishing a current (as corroborated in the right side trace in Fig. 5.) No acoustic signal is detected at this stage of the approach, probably because a fully coalesced meniscus is not formed yet. This situation

remains until the apex reaches z = 35 Å. Upon further approach, the acoustic SANM starts to change more significantly. This is interpreted as the transition from an incipient to a full coalescence of a meniscus between the probe and the sample [25]; hence a more coherent acoustic signal is engendered. This is consistent with the more sustained value of the SANM phase signal recorded for z<35 Å. The probe's amplitude and the damping force experience also a more drastic variation in this last stage of approach.

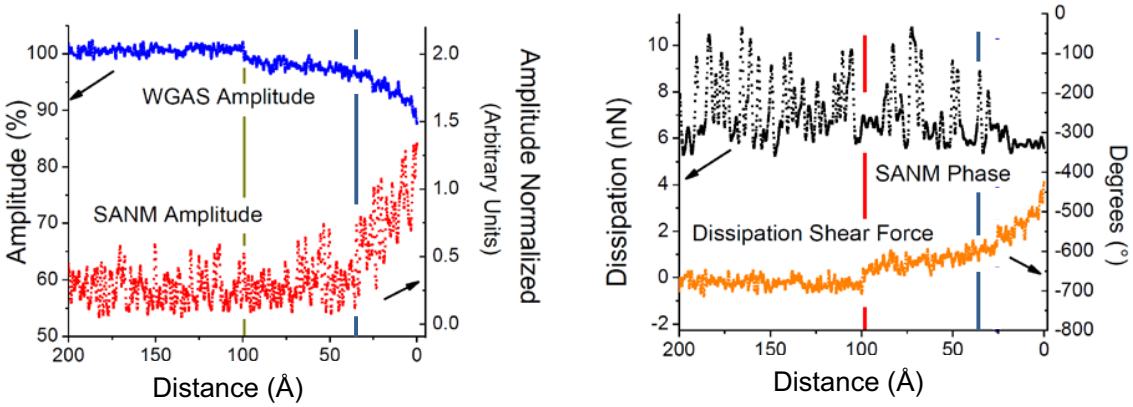

Figure 4 Approach traces. **Left**: WGAS signal (probe's amplitude of oscillations) and SANM amplitude (near-field acoustic emission from the meniscus fluid.) **Right**: Phase of the acoustic SANM signal (a consistent value is obtained only for z < 35 Å) and the damping force acting on the probe. The vertical lines separate regions of no change, small change, and drastic changes in the signals.

Figure 5 shows variations in the current flowing through the water bridge formed between the probe's apex and the substrate. The dashed lines along the contact current traces are to suggest that a different slope characterizes the trace. The greater slope for z < 35 Å is consistent with a denser (coalesced) meniscus bridge, compared to its incipient formation for z > 35 Å. The elastic force exerted by the fluid on the probe (as calculated from expression (17) also increases significantly for z < 35 Å. The traces on the right side show that the probe experiences an increase in its resonance frequency as it approaches the sample, which correlated very well with the elastic force exerted by the fluid on the probe.

Since we associate the generation of an acoustic wave to a non-damping energy dissipation channel of energy involved in the probe-fluid interaction, it is natural then to compare the behavior between the SANM signal and the frequency shift signal, since they correlate with the elastic force measured in these experiments. This is shown in figure 6. The near-field acoustic emission from the fluid, the SANM signal, correlates well with frequency shift experienced by the probe, and the elastic force exerted by the fluid on the probe. Our results support then near-field acoustic emission as one of the elastic energy dissipation channels involved in surface interactions.

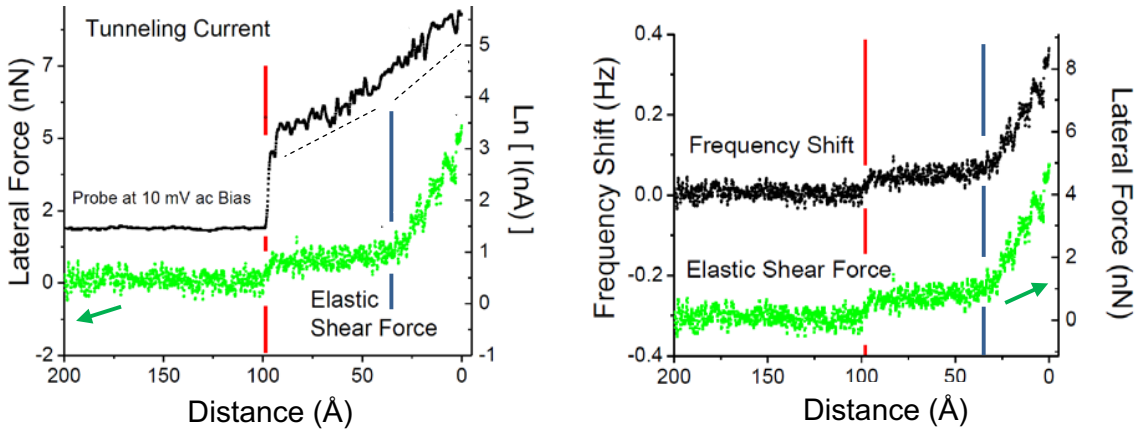

Fig. 5 Approach traces. **Left**: Current through the fluid gap and the elastic force exerted by the fluid on the probe. **Right**: Increase of the probe's resonance frequency compared with the elastic force.

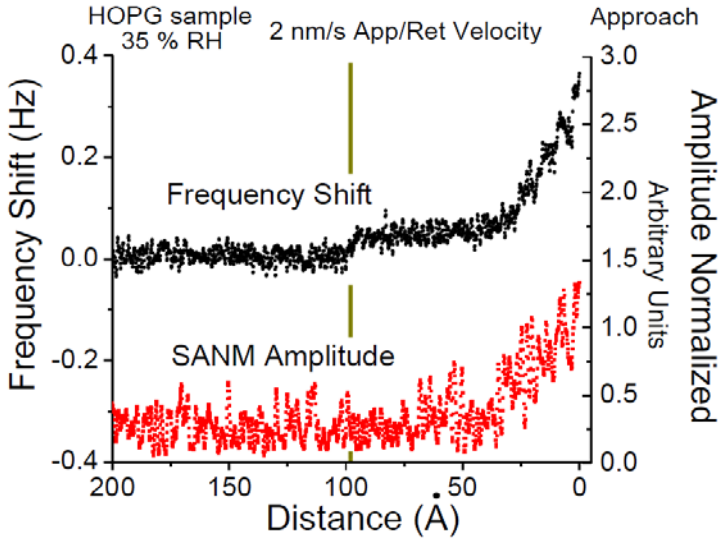

Fig. 6 Traces display a direct correlation between the near-field acoustic emission from the meniscus fluid (SANM signal) and the shift experienced by the probe's resonance frequency, as the probe approaches the sample.

6. Conclusions

Two near-field acoustic techniques, SANM and WGAS were used to characterize the fluid trapped between a sharp probe and a flat solid surfaces at ambient conditions. The lateral motion of the probe, at about 32 kHz and 26 nm amplitude, sets the fluid under shear motion and, as a consequence, causes acoustic emission. SANM is sensitive enough to detect such acoustic waves in the near field region, while WGAS monitors the probe's lateral oscillations amplitude with nanometer-size sensitivity. Implementation of the SANM in frequency modulation modality allowed to discriminate the damping and the elastic component

of the probe-fluid interaction. One of the main findings constitutes the correlation between the SANM acoustic emission from the fluid and the shift in the probe's resonance frequency. The variations of the multiple signals acquired simultaneously (contact current, damping lateral force, elastic lateral force, frequency shift) as the probe approaches the sample were interpreted in term of *i*) first an stochastic formation of incipient bridges between the probe and the substrate, followed by *ii*) the coalescence of a water meniscus, whose effects (on the probe's amplitude and resonance frequency shift are more pronounced as the probe-substrate distance decreases. Overall, the new SANM accounts for an elastic energy dissipation channel in surface interactions.

Acknowledgements

AHLR acknowledges partial support for this work from Lam Research Corporation, CA USA.

Bibliography

[1] Granick S 1991 *Science* **253** 1374
[2] Klein J and Kumacheva E 1995 *Science* **269** 816
[3] Ortiz-Young D, Chiu H -C, Kim S, Voïtchovsky K and Riedo E 2013 *Nat. Commun.* **4** 2482
[4] Jinesh K and Frenken J 2006 *Phys. Rev. Lett.* **96** 166103
[5] Nosonovsky M and Bhushan B 2008 *Phys. Chem. Chem. Phys.* **10** 2137
[6] Jinesh K and Frenken J 2008 *Phys. Rev. Lett.* **101** 036101
[7] Choi E -M, Yoon Y -H, Lee S and Kang H 2005 *Phys. Rev. Lett.* **95** 085701
[8] Hammer M U, Anderson T H, Chaimovich A, Shell M S and J. Israelachvili 2010 *Faraday Discuss.* **146** 299
[9] Voïtchovsky K, Kuna J J, Contera S A, E. Tosatti and F. Stellacci 2010 *Nat. Nanotechnol.* **5** 401
[10] Chiavazzo E, Fasano M, Asinari P and Decuzzi P 2014 *Nat. Commun.* **5** 4565
[11] Duan C and Majumdar A 2010 *Nat. Nanotechnol.* **5** 848
[12] Ahmad M, WGu W, Geyer T and Helms V 2011 *Nat. Commun.* **2** 261
[13] Lv W and Wu R 2013 *Nanoscale* **5** 2765
[14] Huang H, Song Z, Wei N, Shi L, Mao Y, Ying Y, Sun L, Xu Z and Peng X 2013 *Nat. Commun.* **4** 2979
[15] La Rosa A H, Cui X, McCollum J, Li N and Nordstrom R 2005 *Rev. Sci. Instrum.* **76** 093707
[16] Fernandez R, Wang X, and La Rosa A H 2011 *Proceedings of the Nanotechnology* (*IEEE-NANO*) *11th IEEE International Conference* 903.
[17] La Rosa A H, Li N, Fernandez R, Wang X, Nordstrom R and Padigi S K 2011 *Rev. Sci. Instrum.* **82** 093704
[18] Wang X, Fernandez R, Li N, Hung H -C, Venkataraman A, Nordstrom R and La Rosa A H 2016 *Physics of Fluids* **28** 052001.
[19] Karrai K, Grober R D Near Field Optics 1995 in: Paesler M A and Moyer P J (Ed.) 1995 *SPIE Proceedings Series* **2535** Bellingham, WA, pp. 69–81.
[20] Grober R D, Acimovic J, Schuck J, Hessman D, Kindlemann P J, Hespanha J, Morse A S, Karrai K, Tiemann I and Manus S 2000 *Rev. Sci. Instrum.* **71** 2776
[21] Karrai K and Grober R D 1995 *Appl. Phys. Lett.* **66** 1842
[22] An S, Kim J, Lee K, Kim B and Lee M 2012 *Appl. Phys. Lett*. **101** 053114
[23] Karrai K and Tiemann I 2000 *Phys. Rev. B **62*** 13 174-181
[24] Barel I, Filippov A E and MUrbakh M 2012 *J. Chem. Phys.* **137** 164706
[25] Luna M, Colchero J and Baro A M 1998 *Appl. Phys. Lett*. **72** 3461